https://doi.org/10.37434/tpwj2021.10.03

CORROSION-MECHANICAL RESISTANCE OF 2219 ALLOY WELDED JOINTS UNDER SIMULATED SERVICE CONDITIONS*

L.I. Nyrkova[1], **T.M. Labur**[1], **E.I. Shevtsov**[2], **O.P. Nazarenko**[2] and **A.V. Dorofeev**[2]

[1]E.O. Paton Electric Welding Institute of the NASU
11 Kazymyr Malevych Str., 03150, Kyiv, Ukraine
[2]SC «DB Pivdenne»
3 Kryvorizzka Str., 49008, Dnipro, Ukraine

ABSTRACT

We studied the corrosion resistance, including local corrosion resistance, of welded joints of aluminium 2219 alloy, made by nonconsumable electrode single-pass welding along (L) and across (T) the rolled metal heat-treated to the T81 condition. It is shown that resistance of welded joints of 2219 alloy to general and local corrosion in amyl and its vapors does not depend on the direction of workpieces during welding. An increase in ductility and strength values of welded joint specimens was found after soaking them in amyl and amyl vapors. The coefficient of welded joints strength after soaking in amyl rises from 0.65 up to 0.67 in the longitudinal direction, and from 0.64 to 0.66 in the transverse direction. After soaking in amyl vapors, the strength properties of the welded joint almost do not change: strength coefficient was the same in both orientation directions and it was equal to 0.64. Fracture ran along the fusion line of the weld with the base metal, where melting of grain boundaries and their thickening take place during the thermal cycle of welding at crystallization, as well as decomposition of copper over saturated solid solution in aluminium, which is accompanied by precipitation and coagulation of the strengthening phases.

KEY WORDS: 2219 aluminium alloy, welded joints, heat treatment, corrosion resistance, mechanical properties, microstructure, mechanical fracture at tension

Aluminium structural 2219-T31 alloy (USA) belongs to the grade of thermally strengthened alloys of Al–Cu–Mn alloying system, which have a high specific heat capacity. Ultimate strength of wrought heat-treated aluminium alloys can reach 500 MPa and higher at a density lower than 2850 kg/m^3 [1–3]. It belongs to the most used structural materials, in particular, for the manufacture of fuel tanks in various systems of carrier rockets (Saturn V, Apollo, Space Shuttle, etc.).

The specific strength of alloys has high values and is close to the specific strength of high-strength steels. When the temperature decreases, the mechanical properties are not deteriorated and so they are used in a wide temperature range from –250 to +200 °C (at the condition of short-term heating to 250–300 °C). Therefore, the alloy is often used in the structures of cylinders and tanks in which liquid gases are stored. In addition, the alloy is also characterized by technological ductility in the cold and hot state at a high level of corrosion resistance of the metal, which distinguishes this alloy among other structural aluminium alloys [4]. It has a unique combination of physicomechanical and technological properties [1–17]. Its weldability and high strength under cryogenic temperatures are especially valued. Such structures require high ductility in cold and hot states at a high level of corrosion resistance.

2219-T31 alloy belongs to the group of structural materials and to the dispersion-hardened alloys. This alloy contains almost 6 % of copper, and its hardening characteristics are similar to the two-component Al-Cu alloy. The structure of the alloy consists of a solid solution and several phase inclusions: $\Theta'(A1_2Cu)$, $T(Al_{12}Mn_2Cu)$, $A1_3Zr$, $Al_{11}V$, etc., whose presence in the alloy provides a good combination of strength and ductility [18]. Numerous scientific studies indicate the influence of technological conditions of heating, under the action of which structural transformations occur, reduces the indices of mechanical and corrosion properties [1–16]. The degree of their reduction is influenced by the sizes and shape of crystallites and grains of the metal in the heat-affected-zone, the morphology of the distribution of structural components and their number in the volume of the metal. Moreover, the previous deformation has a significant effect, which enhances the action of the mechanism of precipitation of a metastable phase $\Theta'(Al_2Cu)$ and causes the appearance of a stable phase Θ, which initiates the formation of a crack during fracture [14].

*In the work participated: S.O. Osadchuk, M.R. Yavorska, A.G. Poklyatskyi, V.E. Fedorchuk.

Typically, structures of aluminium 2219 alloy, which operate under pressure, are subjected to heat treatment after welding or used in the state of delivery [1]. During heat treatment, various modes are used, including T81 (ageing of workpieces at 177 °C for 18 h in the T4 condition), as well as T87 (ageing of workpieces, heat treated with subsequent deformation of 8 % until the T37 condition, at 163 °C for 24 h).

At the same time, the alloy is very sensitive to temperature effect during welding.Therefore, during melting and crystallization of welds a significant softening of the base material in the HAZ occurs [5, 6]. The morphology of weld microstructure is determined by the temperature gradient on the surface of the distribution of the solid solution of liquid metal and phases, the value of the crystallization rate, as well as the nature of the distribution of alloying elements over the volume of the weld metal. Overheating of the metal causes a decrease in its strength in the HAZ and formation of an inhomogeneous structure as a result of segregation of alloying elements and impurities along the boundaries of crystallites and grains [7–12]. In addition, between the grains brittle interlayers of supersaturated phases appear, especially at the fusion boundary with the base metal, where the interlayers form a dense framework around the grains [14, 15].

Methods of experiments. In the work the aluminium 2219-T31 alloy of the alloying system Al–Cu with a thickness of 3 mm was investigated. The analysis of the chemical composition was performed spectrally in a spectrometer «Spectrovak-1000» of Baird Company. The obtained results were compared with the chemical composition of the alloy given in AMS-QQ-A-250/30A [17] (Table 1). It was found that as to the content of the basic alloying elements and impurities (except for vanadium, the content of which was not determined), the specimen of the investigated semi-finished workpieces of the aluminium alloy meets the requirements of the standard AMS-QQ-A-250/30A.

The plates of 2219-T31 alloy with a size of 300×150×3 mm, cut out along and across to the rolled metal direction were welded. Before welding, the workpieces of the alloy were treated in 10 % NaOH solution and clarified in 30 % HNO_3 solution. Welding of workpieces was performed in a flat position with a nonconsumable tungsten electrode with a lanthanum coating using filler wire of grade 2319 of a diameter 1.6 mm on the conditions: I_w = 280 A, v_w = 20 m/h, filler wire feed rate is 117 m/h. The power source — MW-450 of Fronius Company, an alternating current with a rectangular waveform of 200 Hz frequency was used. The fusion zone was protected with argon. A full penetration of welded edges in a one pass and the formation of the penetration (root) was achieved in the presence of a removable stainless steel backing with a rectangular groove of 4 mm width and 1 mm depth, which allowed obtaining a high-quality formation of butt joints with appropriate technological reinforcement.

The quality of weld formation of butt joints of 2219-T31 alloy was evaluated visually and using radiography method (GOST 7512 [18]) in the RAP-150/300 installation. The density of the weld metal was tested in the DP-30 densitometer.

To measure geometric parameters of the welds, an electronic caliper of grade ART-34460-150 with a graduation mark of 0.01 mm was used.

The specimens for mechanical and corrosion tests were made from welded billets in accordance with the relevant standard documents. The specimens of welded joints were heat treated to the T81 condition (artificial ageing) on the mode: $T = 180 \pm 5$ °C during 18 h.

Corrosion tests were performed in amyl and amyl vapors at a temperature of 50 °C continuously during 45 days on the base of the testing laboratory of the DB «Pivdenne». Then, the corrosion resistance (general corrosion rate, resistance to MCC, exfoliating corrosion and corrosion cracking) as well as mechanical properties were evaluated. Evaluation of the resistance of the base metal specimens to continuous corrosion was performed by the massometry method in accordance with GOST 9.908 [19]. The rate of weight loss of the specimens was determined by the change in their mass and duration of corrosion studies by the formula:

$$K = \frac{\Delta m}{ST}, \quad (1)$$

where $\Delta m = m_1 - m_2$ are corrosion losses of the specimen, g; m_1 is the mass of the specimen before the tests, g; m_2 is the mass of the specimen after the corro-

Table 1. Results of analysis of chemical composition of specimen of 2219-T31 alloy with a thickness of 3 mm

Reference specimen, or standard requirements	Mass fraction of elements, %									
	Cu	Mn	Zr	V	Ti	Fe	Si	Zn	Mg	Other elements: each one/in general
Specimen	6.7	0.34	0.18	–	0.05	0.16	0.09	0.03	0.02	0.01 (Ni)
AMS-QQ-A-250/30A	5.8–6.8	0.20–0.40	0.10–0.25	0.05–0.15	0.02–0.10	≤0.30	≤0.20	≤0.10	≤0.02	≤0.05/≤0.15

sion tests; S is the surface area of the specimen, m^2; T is the duration of investigations, h.

The corrosion rate was calculated by the formula:

$$\Pi = \frac{8760K}{d}, \quad (2)$$

where K is the corrosion rate, g/(m²·h); d is the metal density, g/cm³; 8760 is the number of hours per year.

The density of aluminium alloys is 2.7 g/cm³, which was taken into account during calculation.

The evaluation of resistance to exfoliating corrosion was carried out on the specimens of the base metal and welded joints according to GOST 9.904 [20]. While evaluating the condition of the experimental specimens, the change of colour, presence of ulcers and exfoliations on the working surfaces of the specimens and cracks on the ends were noted. The following symbols were taken. The letter «A» indicates the surface, on which marking is applied, and for the welded joints it indicates the surface with a facial weld, B indicates the back surface and for the welded joints it means the surface with penetration; *1*, *2* — ends of the sides with the length of 60 mm (80 mm for welded joints), *3*, *4* — ends of sides with the length of 40 mm (25 mm — for welded joints).

The evaluation of resistance of the alloy to MCC was carried out by a metallographic method at a magnification ×(100–200) according to GOST 9.021 [21] on the specimens of welded joints, all structural zones of the welded joint were evaluated, namely: base metal, heat-affected-zone and weld.

The tests of resistance to corrosion cracking were carried out on rectangular specimens with the size of 150.0×25.0×3.0 mm. The specimens were loaded according to a four-point bending scheme according to GOST 9.901.2 (method 4), the level of continuous deformation was agreed with the SE DB «Pivdenne» and amounted to 957 kgf/cm². The presence (absence) of cracks was revealed visually by means of a magnification glass.

The determination and evaluation of mechanical properties was performed on the plane specimens with technological reinforcement on the facial and back surfaces of the weld. Mechanical tests were carried out in accordance with GOST 1497 [22] in the Instron-1126 machine at a speed of traverses movement of 6 mm/min until fracture. To monitor the indice of relative elongation of the specimens, an extensometer No.G-51-12-M-A was used. During the tests with the help of a personal computer, the values of load and deformation were continuously recorded, according to the results of which, yield strength, ultimate tensie stength and relative elongation were calculated.

Metallographic analysis of the base metal and welded joints before and after corrosion tests was performed by means of a microscope MMT-1600V. The studies were conducted on the sections cut out from the butt joints, welded along (L) and across (T) the rolled sheet semifinished product. The microstructure was detected by etching in the solution of such composition: chloric acid — 1000 cm³ + ice acetic acid — 75 cm³.

Results and their discussion. *Geometric parameters of welds.* After welding butts, geometric parameters of produced welds were determined (B is the width of a weld from a facial surface of joints, H is the width of a weld from a back surface of joints (weld root); δ is the penetration depth of the base metal (in this case it is equal to its thickness); b is the height of convexes of technological reinforcement, h is the height of weld root). According to the results of measurements, the width of welds in the joints of 2219-T31 alloy cut out along the rolled metal, amounts from 9.56 to 9.72 mm, and across the rolled metal it is from 9.47 to 9.65 mm. The weld factor according to the formula $K = B/(b + \delta)$ for the joints welded along and across the rolled metal by nonconsumable electrode, is equal to 2.13 and 2.03, respectively.

Investigation of resistance to general and local corrosion. After the tests, a nonuniform darkening of surface of the specimens (Figure 1) and formation of corrosion spots of various sizes from 20 to 40 % was observed. After the contact with amyl vapors, darkening of the surface was also nonuniform, the area of corrosion spots amounted from 10 to 20 %. The spots are characterized by a change in colour of the surface layer (darkening) and a small depth of damage.

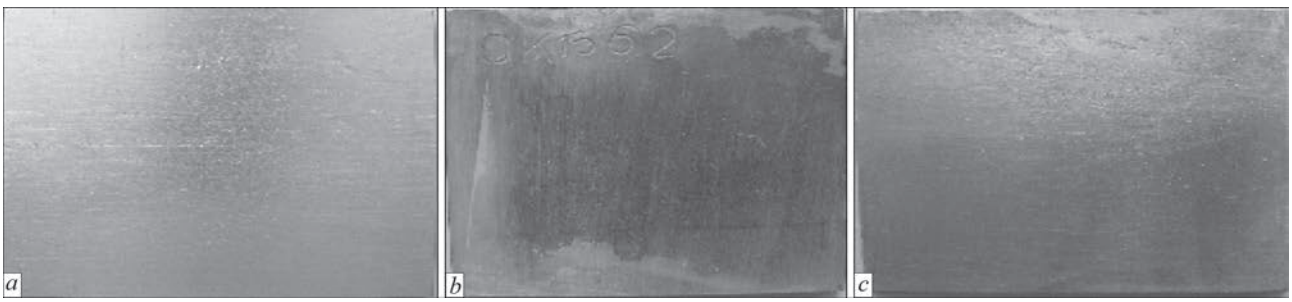

Figure 1. Appearance of base metal surface of aluminium 2219 alloy, heat-treated to the T81 condition, before (*a*) and after tests in amyl (*b*) and amyl vapors (*c*)

Table 2. Results of evaluation of resistance to exfoliating corrosion of base metal specimens of 2219-T31 alloy and welded joints produced along (L) and across (T) the rolled metal, as well as heat-treated to the T81 condition, after staying in amyl and its vapors

Marking	Rolled metal direction	Corrosion test conditions	Indice description										
			Nature of change in the appearance of specimens		Largest diameter of exfoliating, mm		Exfoliating area on each surface, %		Total length of ends with cracks, mm				Resistance to exfoliating corrosion according to GOST 9.904, point
			A	B	A	B	A	B	1	2	3	4	
Base metal	L	Amyl	Slight darkening		0	0	0	0	0	0	0	0	2
		Amyl vapors	Change of color by spots. Slight darkening. Spots with temper colors		0	0	0	0	0	0	0	0	2
		Ref.	Without changes		0	0	0	0	0	0	0	0	1
Welded joint	L	Amyl	Slight darkening. Spots with temper colors		0	0	0	0	0	0	0	0	2
		Amyl vapors	Slight darkening		0	0	0	0	0	0	0	0	2
		Ref.	Without changes		0	0	0	0	0	0	0	0	1
Base metal	T	Amyl	Slight darkening. Spots with temper colors		0	0	0	0	0	0	0	0	2
		Amyl vapors	Same		0	0	0	0	0	0	0	0	2
		Ref.	Without changes		0	0	0	0	0	0	0	0	1
PCK.11.81	T	Amyl	Slight darkening		0	0	0	0	0	0	0	0	2
PCK.13.81		Amyl vapors	Same		0	0	0	0	0	0	0	0	2
PCK.15.81		Ref.	Without changes		0	0	0	0	0	0	0	0	1

After removing the corrosion products, the surfaces are brilliant, local corrosion damages of the surface were not detected. According to the results of visual examination, after the tests in amyl environment (liquid and vapors), corrosion of aluminium 2219 alloy was identified according to GOST 9.908 as a continuous nonuniform, type of damages — corrosion spots. High-speed indices of continuous corrosion of the specimens of the base metal of aluminium 2219 alloy in the T81 condition, determined in accordance with GOST 9.908, are the following: weight loss rate in amyl is 0.00111 g/(m^2·h), in amyl vapors they are 0.00346 g/(m^2·h); linear rate of corrosion in amyl is 0.00362 mm/year, in amyl vapors it is 0.01120 mm/year.

Thus, to some extent amyl vapors are more corrosion-aggressive relative to the aluminium 2219 alloy as compared to liquid amyl: the rate of corrosion in the amyl vapors grows by 3.1 times as compared to amyl. According to a ten-point scale of corrosion resistance according to GOST 9.502 [23], the resistance of aluminium 2219 alloy, heat-treated to the T81 condition, in amyl is evaluated by a point 2, in amyl vapors it has a point 4, which corresponds to the group of metal resistance «highly resistant» and «resistant», respectively.

According to the evaluation results, it was found (Table 2) that resistance of the base metal of 2219 alloy to the exfoliating corrosion after the tests in amyl and its vapors and welded joints along (L) and across (T) the rolled metal, heat-treated to the T81 condition, corresponds to the point 2 according to GOST 9.904.

Thus, ressitance of welded joints of the base metal to exfoliating corrosion in amyl and its vapors does not affect the direction of a rolled semifinished product and the thermal cycle of welding.

After the corrosion tests in amyl and its vapors, the fracture of welded joints of 2219 alloy along the grain boundaries was not detected, and these joints are resistant to intercrystalline corrosion in accordance with GOST 9.021. Their resistance is not affected by the direction of rolled metal and thermal cycle of welding. The specimens of welded joints of 2219 alloy along (L) and across (T) the rolled metal in the T81 condition are resistant also to corrosion cracking in amyl and its vapors.

The welded joints of 2219 alloy along (L) and across (T) the rolled metal in the T81 condition are resistant to intercrystalline corrosion and corrosion cracking in amyl and its vapors. Resistance to exfoliating corrosion is evaluated by the point 2, the rate of corrosion of the base metal in amyl is 00362 mm/year, in vapors it is 0.01120 mm/year. Their resistance is not affected by the direction of rolled metal and thermal cycle of welding.

Examination of microstructure. Metallographic analysis of the microstructure of the base metal of 2219-T31 alloy showed that its morphology consists of α-phase enriched with aluminium (solid solution) and a stable θ($CuAl_2$)-phase. To the intermediate phases θ′($CuAl_2$) and S′(Al_2CuMg) belong. The main alloying elements are copper and manganese. The presence of

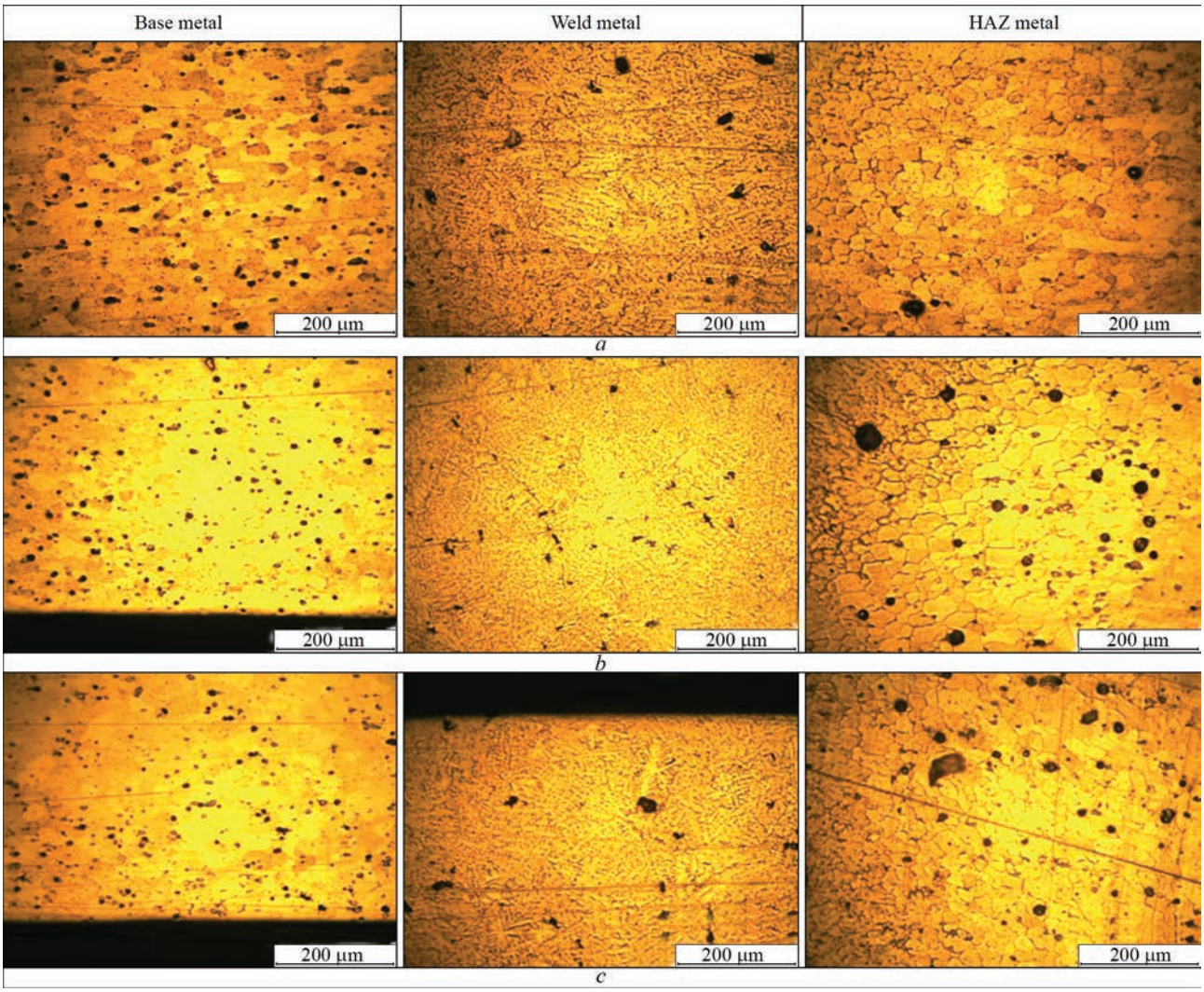

Figure 2. Microstructure of welded joints of aluminium 2219 alloy, heat-treated to the T81 condition, along (L) the rolled metal before corrosion tests (*a*), after tests in amyl environment (*b*) and its vapors (*c*)

the phases θ(Al_2Cu), T($Al_{12}Mn_2Cu$) and $A1_3Zr$, $A1_{11}V$ in the structure of the alloy provides a proper level of physical and mechanical properties of both the alloy itself and its welded joints. This is predetermined by a characteristic special mechanism of decomposition of a solid solution and the morphology of the location of phase precipitates during heating, as well as the ratio of their volumetric density in the structure. The number of phase components is determined by the total amount of alloying elements for a specific alloy.

The structure of the base metal of 2219 alloy in the T81 condition before the corrosion tests is characterized by the presence of grains of a solid solution of the main alloying elements in aluminium. Grains have an elongated shape along the direction of the rolled metal. In the volume of the alloy, precipitates of saturated phases are observed that contain the main alloying element of the alloy — copper. Nonmetallic inclusions are uniformly located over the whole metal cross-section (Figure 2). Signs of macro- and microchemical heterogeneity in structural components are not observed, indicating a high quality of the examined alloy.

In the specimens cut out in the longitudinal direction (Figure 2), along the rolled semifinished product, the length of grains is in average 60 μm, and the width is 35 μm (perpendicular to the thickness of the sheets). In a transverse direction, the size of grains is 60×35 μm, indicating the absence of anisotropy of the metal not only relative to a semifinished product, but also over the thickness (Figure 3).

A more thorough study of the structural features by the method of optical microscopy in a dark field showed that dark inclusions of irregular shape, which are uniformly located in the volume of the alloy, are intermetallic phases. A part of the inclusions has a spherical shape with a maximum size of about 12 μm. Taken into account their size, these intermetallics precipitated from a solid solution during heat treatment of the specimens. Other phase inclusions have a more elongated oval shape with a maximum size of 35×12 μm. They are not dissolved during arc welding and were formed

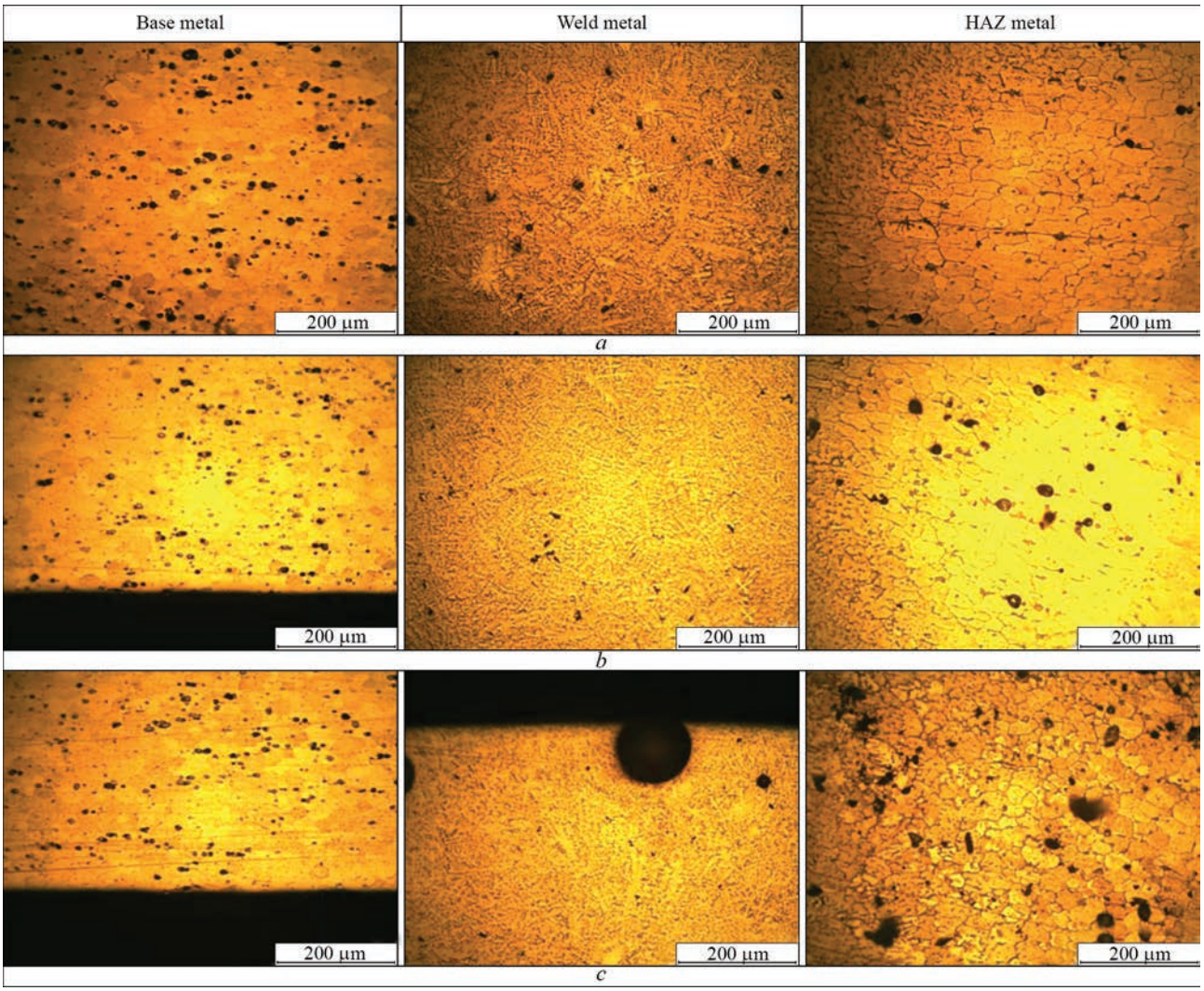

Figure 3. Microstructure of zone of welded joints of aluminium 2219 alloy, heat-treated to the T81 condition across (T) the rolled metal before corrosion tests (*a*), after tests in amyl environment (*b*) and its vapors (*c*)

at the metallurgical stage of manufacturing semifinished products and acquired an elongated shape in the process of plastic deformation in the sheets.

In the structure of welded joints, the zones can be distinguished, that differ from each other. Cast metal is observed in the welds. It has a dendritic structure. In the center of the weld, dendrites are located along the direction of welding. Directly near the fusion boundary of the weld with the base metal, dendrites have a columnar structure and directed from the fusion line to the center of the weld crystallization. Along the dendrites boundaries, the precipitates of eutectic origin (Figures 2, 3) are present, which have a size of not more than 15 μm. A uniform porosity is observed, typical to alloys of this alloying system. The size of pores does not exceed 50 μm. Their density is 7–12 pcs per 1 mm^2. On separate areas of the weld, single pores of up to 0.4 mm were detected, which is admissible according to DSTU EN ISO 10042 [14].

The fusion line separates the weld metal, which was completely melted during welding, from the base metal, which completely or partially remains in a solid state. It can not always be clearly determined, but it separates dendritic structure of the cast weld metal and the grain structure of the deformed HAZ metal (Figures 2, 3).

In HAZ intensive recrystallization processes were not detected. The size of the grains in this zone is not significantly different from the grains of the base metal. At the same time, precipitation of low-melting eutectics along the boundaries of grains is observed, which is associated with the redistribution of alloying elements between the structural components of the alloy under the influence of heating the HAZ metal to the temperatures higher than the solidus temperature (Figures 2, *c* and 3, *c*). This leads to the fact that in the HAZ near the fusion line the structure is formed characteristic to the state of heat treatment of alloys called «overburning» and is accompanied by a decrease in hardness (Figure 4).

This structural area is an integral part of any welded joint of aluminium alloys produced by fusion welding. At the distance from the fusion line to the base metal, the areas of annealing and over-

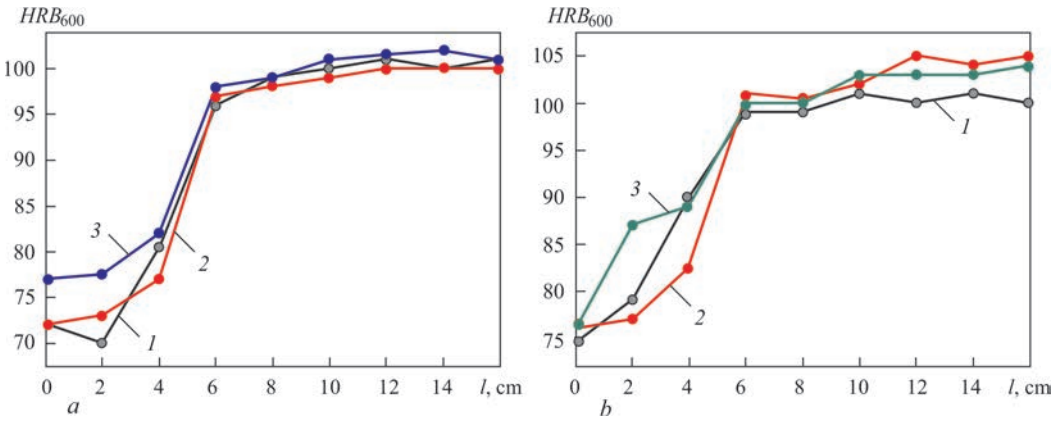

Figure 4. Nature of distribution of hardness over different zones of welded joint of 2219 alloy in the T81 condition along (*a*) and across (*b*) the rolled metal before corrosion tests (*1*), after corrosion tests in amyl environment (*2*) and its vapors (*3*)

ageing are also present, formed under the influence of heat of the welding arc. In these areas, as a result of coagulation processes, intermetallic phase precipitates are observed, which are increased up to 25 μm. The total width of the HAZ of the specimens of welded joints in the T81 condition is 6 mm. In the specimens, welded along and across the rolled metal, significant differences in the width of the HAZ area were not detected.

After the corrosion tests in amyl (Figures 2, 3, *b*) and amyl vapors (Figures 2, 3, *c*), any changes in the microstructure and grain size in the base metal, weld metal and HAZ are not observed.

Investigation of the mechanical properties. Figure 5 shows the averaged values of indices of mechanical properties: tensile strength, yield strength and relative elongation (Figure 5). The value of yield strength ($\sigma_{0.2}$) of the reference specimens of the base metal, cut out along the direction of the rolled metal (Figure 5, *a*), amounts from 365 to 367 MPa, and the tensile strength σ_t is from 462 to 463 MPa (Figure 5, *b*). In the specimens cut out in a transverse direction $\sigma_{0.2}$ is 362–365 MPa (Figure 5, *c*), σ_t is 468–469 MPa (Figure 5, *d*), which is slightly higher than for the specimens cut in the longitudinal direction.

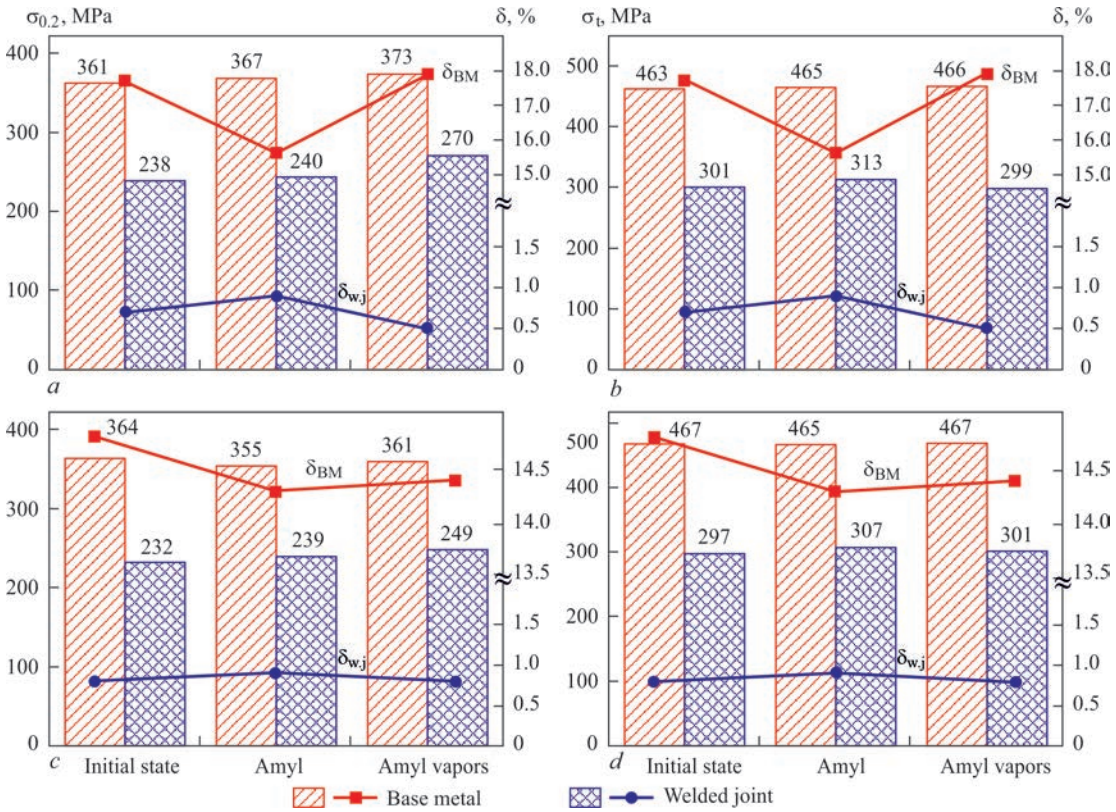

Figure 5. Mechanical properties of base metal and welded joint of 2219 alloy in the T81 condition along (*a*, *b*) and across (*c*, *d*) the rolled metal before corrosion tests and after corrosion tests in amyl and its vapors. Columns are tensile and yield strength, line is relative elongation

An analysis of the results of tests of the reference specimens of the welded joints, welded along the rolled metal, showed that the yield strength decreased by about 34–36 % as compared to the base metal — to 234–241 MPa (Figure 5, *a*). The tensile strength of the welded joints is 293–308 MPa (Figure 5, *b*), which is by 33–37 % lower than the strength of the base metal. The strength coefficient of the reference specimens of the welded joints is equal to 0.65.

A similar pattern was observed for the specimens of welded joints made across the direction of the rolled metal. The values of the yield strength of the reference specimens of welded joints was 229–234 MPa (Figure 5, *c*), which is approximately by 36–37 % lower than of the base metal. The tensile strength of the welded joints was from 271 to 323 MPa, which is lower than the strength of the base metal by approximately 31–45 %. The strength coefficient of the reference specimens of the welded joints, made across the rolled metal, was equal to 0.64.

After the tests of the specimens in amyl, the values of the yield strength of the base metal of 2219-T81 alloy in the longitudinal direction increased by almost 3 % and amounted from 355 to 373 MPa. At the same time, the level of strength increased by 1 % — 464–466 MPa. Soaking of the specimens in amyl vapors also caused an increase in yield stregnth by 4–5 % — up to 371–374 MPa and tensile strength by 1 % — up to 465–467 MPa.

After the corrosion tests of the specimens of joints, welded along the direction of the rolled metal, in amyl an increase in the value of the yield strength by ~1 % to 230–257 MPa (Figure 5, *a*) was observed. The tensile strength of the joints increased by ~4 %, to 309–315 MPa (Figure 5, *b*), indicating strengthening of the phase components of the metal structure after the contact with amyl. The tests of the longitudinal specimens of the welded joints in the amyl vapors contributed to an increase in the yield strength by ~13 % (up to 261–271 MPa), but a slight decrease in strength by ~1 % (to 290–308 MPa) (Figure 5, *a*, *b*).

The specimens of the base metal, cut out in the transverse direction relative to the rolled metal after soaking in amyl have the following properties: yield strength is 352–357 MPa, tensile strength is 465–467 MPa, i.e., both indices slightly decreased as compared to the indices for the specimens in the initial state. After the tests in amyl vapors, the yield strength decreased slightly (to 353–370 MPa), tensile strength did not change and amounted to 466–468 MPa.

In the specimens, welded across the direction of the rolled metal, after the action of amyl, the value

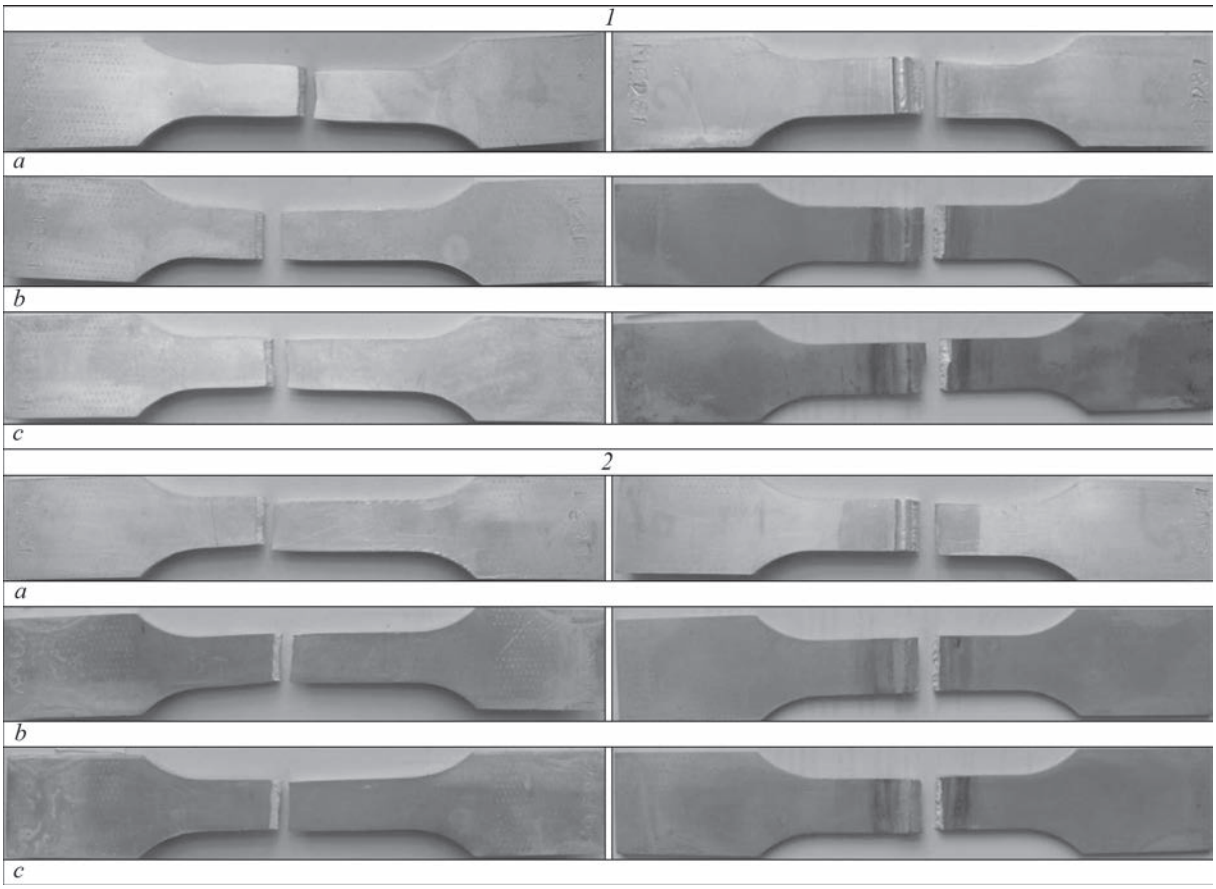

Figure 6. Appearance of base metal and welded joint of 2219 alloy specimens in the T81 condition along (*1*) and across (*2*) the rolled metal before corrosion tests (*a*), after corrosion tests in amyl (*b*) and its vapors (*c*)

of yield strength was 226–251 MPa (Figure 5, *c*), which was little different from the yield strength of the welded joints, produced along the rolled metal, but was lower than in the base metal. A similar pattern was observed for the tensile strength of these welded joints — 301–313 MPa (Figure 5, *d*).

The exposure of the specimens of joints welded in a transverse direction, in the amyl vapors contributed to a decrease in the yield strength to 254–261 MPa, and almost did not affect the value of the tensile strength, which was equal to 298–305 MPa.

The strength coefficient of the welded joints after the tests in amyl increased a bit as compared to the base metal and was 0.67 for the specimens welded along the rolled metal, and 0.66 for the transverse specimens.

For the specimens welded in the longitudinal direction, after the effect of amyl vapors, a decrease in relative elongation from 0.7 to 0.5 % was noted, for the transverse specimens, this indice did not changed and amounted to 0.8 %. The strength coefficient of the welded joints both for longitudinal specimens and transverse specimens after the action of amyl vapors was the same and amounted to 0.64.

The fracture of all the investigated specimens of welded joints of 2219 alloy occurred along the fusion line of the weld with the base metal (Figure 6), where during the thermal cycle of welding, grain boundaries are flashed and decomposition of an oversaturated solid solution of copper in aluminium occurs. Such structural changes are accompanied by precipitation and coagulation of strengthening phases, which causes thickening of grain boundaries.

As is evidenced by the analysis of the surface of fractures of the broken specimens of welded joints of the alloy, regardless of the direction of the rolled metal of semifinished products, their reliefs have a predominantly skewed character with a tough cell structure, the formation of which is accompanied by significant plastic deformations of the specimen material. The center of microcracking is the inclusions of intermetallic phases, which remain in the metal in the process of manufacturing semifinished products and do not dissolve in the conditions of arc welding.

CONCLUSIONS

1. Welded joints of aluminium 2219 alloy, made by single-pass nonconsumable electrode welding along (L) and across (T) the rolled metal, heat-treated to the T81 condition, are resistant to corrosion cracking and intergranular corrosion. The resistance to exfoliating corrosion in amyl and its vapors is evaluated by the point 2. According to a ten-point scale in accordance with GOST 9.502, the corrosion resistance of the base metal of the aluminium 2219 alloy in the T81 condition in amyl is evaluated by a point 2, which corresponds to the resistance group «highly resistant»; in amyl vapors — by a point 4, which corresponds to the resistance groups «resistant».

2. The resistance of welded joints of 2219 alloy to general and local corrosion in amyl and its vapors is not affected by the direction of welding process of semifinished products relative to the rolled metal and thermal welding conditions.

3. After soaking in amyl and amyl vapors, the ductility and strength indices of the welded joint specimens increase as compared to similar indices before the corrosion tests. The strength coefficient of the welded joints in the longitudinal direction after soaking in amyl is equal to 0.67, in the transverse direction it is 0.66, and after the action of amyl vapors for the joints welded in the longitudinal and transverse directions are the same and amount to 0.64. All the experimental specimens of welded joints of the alloy are fractured along the fusion line of the weld with the base metal, where during the thermal cycle of welding, a decomposition of an oversaturated solid solution of copper in aluminium and flashing of grain boundaries and coagulation of strengthening phases occur. This is accompanied by thickening of grain boundaries as a result of precipitation of phases during crystallization. Irrespective of the direction of welding relative to the rolled metal, its fractures of the experimental specimens during their breaking have a tough nature of the relief.

The work was performed with the support of SE «DB Pivdenne» (state registration number 011811006291s) in 2018.

REFERENCES

1. Rao, P.S., Sivadasan, K.G., Balasubramanian, P.K. (1996) Structure-property correlation on AA 2219 aluminium alloy workpieces. *Bulletin of Materials Sci.*, 19(**3**), 549–557.
2. Li, H., Zou, J., Yao, J., Peng, H. (2017) The effect of TIG welding techniques on microstructure, properties and porosity of the welded joint of 2219 aluminium alloy. *J. of Alloys and Compounds*, **727**, 531–539.
3. Zhang, D., Wang, G., Wu, A. et al. (2019) Study on the inconsistency in mechanical properties of 2219 aluminium alloy TIG-welded joints. *J. of Alloys and Compounds*, **777**, 1044–1053.
4. Grilli, R., Baker, M.A., Castle, J.E. et al. (2010) Localized corrosion of a 2219 aluminium alloy exposed to a 3.5 % NaCl solution. *Corrosion Sci.*, 52(**9**), 2855–2866.
5. Zhang, D., Wu, A., Zhao, Y. et al. (2021). Effects of the number of welding passes on microstructure and properties of 2219-C10S aluminium alloy TIG-welded joints. *J. of Mater. Eng. and Performance*, **5**, 3537–3546.
6. Wan, Z., Meng, D., Zhao, Y. et al. (2021) Improvement on the tensile properties of 2219-T8 aluminium alloy TIG welding joint with weld geometry optimization. *J. of Manufacturing Processes*, **67**, 275–285.

7. Niu, L.Q., Li, X.Y., Zhang, L. et al. (2017) Correlation between microstructure and mechanical properties of 2219-T8 aluminium alloy joints by VPTIG welding. *Acta Metallurgica Sinica*, 30(**5**) 438–446.
8. Zhang, D.K., Wang, G.Q., Wu, A.P. et al. (2019) Effects of post-weld heat treatment on microstructure, mechanical properties and the role of weld reinforcement in 2219 aluminium alloy TIG-welded joints. *Acta Metallurgica Sinica*, 32(**6**), 684–694.
9. Gupta, R.K., Panda, R., Mukhopadhyay, A.K. et al. (2015) Study of aluminium alloy AA2219 after heat treatment. *Metal Sci. and Heat Treatment*, 57(**5**), 350–353.
10. Lu, Y., Wang, J., Li, X. et al. (2018) Effects of pre-deformation on the microstructures and corrosion behavior of 2219 aluminium alloys. *Mater. Sci. and Engin.: A*, **723**, 204–211.
11. Chen, S., Li, F., Liu, Q. et al. (2020) Effect of post-aging heat treatment on strength and local corrosion behavior of ultrafine-grained 2219 Al alloy. *J. of Mater. Engin. and Performance*, 29(**5**), 3420–3431.
12. Zhang, D., Li, Q., Zhao, Y. et al. (2018) Microstructure and mechanical properties of three-layer TIG-welded 2219 aluminium alloys with dissimilar heat treatments. *Ibid.*, 27(**6**), 2938–2948.
13. Zhu, Z.Y., Deng, C.Y., Wang, Y. et al. (2015) Effect of post weld heat treatment on the microstructure and corrosion behavior of AA2219 aluminium alloy joints welded by variable polarity tungsten inert gas welding. *Materials & Design (1980–2015)*, **65**, 1075–1082.
14. Peng, X.N., Qu, W.Q., Zhang, G.H. (2009) Influence of welding processes on mechanical properties of aluminium alloy 2219. *J. of Aeronautical Materials*, **2**, 57–60.
15. Bai, J.Y., Yang, C.L., Lin, S.B. et al. (2016) Mechanical properties of 2219-Al components produced by additive manufacturing with TIG. *The Int. J. Adv. Manuf. Technol.*, 86(**1**), 479–485.
16. Rao, S.K., Reddy, G.M., Rao, K.S. et al. (2005) Reasons for superior mechanical and corrosion properties of 2219 aluminium alloy electron beam welds. *Materials characterization*, 55(**4–5**), 345–354.
17. AMS-QQ-A-250/30A. *Specifications. Aluminium alloy 2219. Sheet and plate* [in Ukrainian].
18. GOST 7512–82: *Nondestructive testing. Welded joints. Radiography method* [in Ukrainian].
19. GOST 9.908–85: *Unified system of corrosion and ageing protection. Metals and alloys. Methods for determination of corrosion and corrosion resistance indices* [in Russian].
20. GOST 9.904–82: *Unified system of corrosion and ageing protection. Aluminium alloys. Accelerated test method for exfoliating corrosion* [in Russian].
21. GOST 9.021–74: *Unified system of corrosion and ageing protection. Aluminium and aluminium alloys. Accelerated test method for intercrystalline corrosion* [in Russian].
22. GOST 1497–84 (ISO 6892-84, CT CMEA 471-88) *Metals. Methods of tension test* [in Russian].
23. GOST 9.502–82 (CT CMEA 6194–88): *Unified system of corrosion and ageing protection. Inhibitors of metals corrosion for aqueous systems. Methods of corrosion tests (with modifications Nos 1, 2)* [in Russian].

ORCID
L.I. Nyrkova: 0000-0003-3917-9063,
T.M. Labur:0000-0002-4064-2644

CONFLICT OF INTEREST
The Authors declare no conflict of interest

CORRESPONDING AUTHOR
L.I. Nyrkova
E.O. Paton Electric Welding Institute of the NASU
11 Kazymyr Malevych Str., 03150, Kyiv, Ukraine
E-mail: lnyrkova@gmail.com

SUGGESTED CITATION
L.I. Nyrkova, T.M. Labur, E.I. Shevtsov, O.P. Nazarenko and A.V. Dorofeev (2021) Corrosion-mechanical resistance of 2219 alloy welded joints, under simulated service conditions. *The Paton Welding J.*, **10**, 18–27.

JOURNAL HOME PAGE
https://pwj.com.ua/en

Received 27.08.2021
Accepted: 11.11.2021